

# QARC: Video Quality Aware Rate Control for Real-Time Video Streaming based on Deep Reinforcement Learning

Tianchi Huang<sup>†\*</sup>, Rui-Xiao Zhang<sup>\*</sup>, Chao Zhou<sup>‡</sup>, and Lifeng Sun<sup>\*</sup>

<sup>\*</sup> Department of Computer Science and Technology, Tsinghua University, Beijing, China

<sup>‡</sup> Beijing Kwai Technology Co., Ltd, China

<sup>†</sup> Department of Computer Science and Technology, Guizhou University, Guizhou, China

{htc17,zhangrx17}@mails.tsinghua.edu.cn

zhouchaoyf@gmail.com, sunlf@mail.tsinghua.edu.cn

## ABSTRACT

Real-time video streaming is now one of the main applications in all network environments. Due to the fluctuation of throughput under various network conditions, how to choose a proper bitrate adaptively has become an upcoming and interestingly issue. To tackle this problem, most adaptive bitrate control methods have been proposed to provide high video bitrates instead of video qualities. Nevertheless, we notice that there exists a trade-off between sending bitrate and video quality, which motivates us to focus on how to get a balance between them.

In this paper, we propose QARC (video Quality Awareness Rate Control), a rate control algorithm that aims to have a higher perceptual video quality with possibly lower sending rate and transmission latency. Starting from scratch, QARC uses deep reinforcement learning(DRL) algorithm to train a neural network to select future bitrates based on previously observed network status and past video frames. To overcome the “state explosion problem”, we design a neural network to predict future perceptual video quality as a vector for taking the place of the raw picture in the DRL’s inputs.

We evaluate QARC over a trace-driven emulation, outperforming existing approach with improvements in average video quality of 18% - 25% and decreases in average latency with 23% -45%. Meanwhile, Comparing QARC with offline optimal high bitrate method on various network conditions also yields a solid result.

## CCS CONCEPTS

• **Information systems** → *Multimedia streaming*; • **Computing methodologies** → *Neural networks*;

## KEYWORDS

Real-time Video Streaming, Rate Control, Reinforcement learning, Quality-Rate

## ACM Reference Format:

Tianchi Huang<sup>†\*</sup>, Rui-Xiao Zhang<sup>\*</sup>, Chao Zhou<sup>‡</sup>, and Lifeng Sun<sup>\*</sup>. 2021. QARC: Video Quality Aware Rate Control for Real-Time Video Streaming based on Deep Reinforcement Learning. In *Proceedings of ACM Conference (Conference’17)*, Jennifer B. Sartor, Theo D’Hondt, and Wolfgang De Meuter (Eds.). ACM, New York, NY, USA, Article 4, 11 pages. [https://doi.org/10.475/123\\_4](https://doi.org/10.475/123_4)

## 1 INTRODUCTION

Recent years have seen a rapid increase in the requirements of real-time video streaming. People publish and watch live video streaming using different applications(e.g., Twitch, Kwai, Douyu) at any time, in anywhere, and especially, in any network environments. Due to the complicated environment and stochastic property in various network environments, transmitting video stream with high video bitrate and low latency has become the fundamental challenge in real-time live video streaming scenario. Most rate control approaches have been proposed to tackle the problem, e.g. loss-based approach (TFRC [11], RAP [22]), delay-based approach (Vegas [2], LEDBAT (Over UDP) [25]), and QoE-based approach (Google Congestion Control(GCC) [3], Rebera [15]). The same strategy of them is to select bitrate as high as possible with the permission of network condition. However, due to the inequality between high video quality and high bitrate, this strategy may cause a large waste of bandwidth resources. For example, if a video footage consists of darkness and few objects, a low bitrate may also provide a barely satisfactory perceptual video quality but can save large bandwidth resources, and the example is shown in Figure 1(a).

In our study, we propose QARC(video Quality Awareness Rate Control), a novel deep-learning based rate control algorithm aiming to get high video quality and low latency. Due to that fixed rules fail to effectively handle the complicated scenarios caused by perplexing network conditions and various video content, we use DRL to select the future video bitrate, which can adjust itself automatically to the variety of its inputs. In details, QARC uses DRL method to train a neural network to select the bitrate for future video frames based on past time network status observed and historical video frames. However, if we directly import raw pictures as the inputs of state, the state space will cause “state explosion” [5]. To tackle these challenges, we meticulously divide this complexed RL model into two feasible and useful models: one is Video Quality Prediction Network (VQPN), which can predict future video quality via previous video frames; the other is Video Quality Reinforcement Learning (VQRL). VQRL uses A3C [18], an RL method, to train the

Permission to make digital or hard copies of part or all of this work for personal or classroom use is granted without fee provided that copies are not made or distributed for profit or commercial advantage and that copies bear this notice and the full citation on the first page. Copyrights for third-party components of this work must be honored. For all other uses, contact the owner/author(s).  
Conference’17, July 2017, Washington, DC, USA  
© 2021 Copyright held by the owner/author(s).  
ACM ISBN 123-4567-24-567/08/06...\$15.00  
[https://doi.org/10.475/123\\_4](https://doi.org/10.475/123_4)

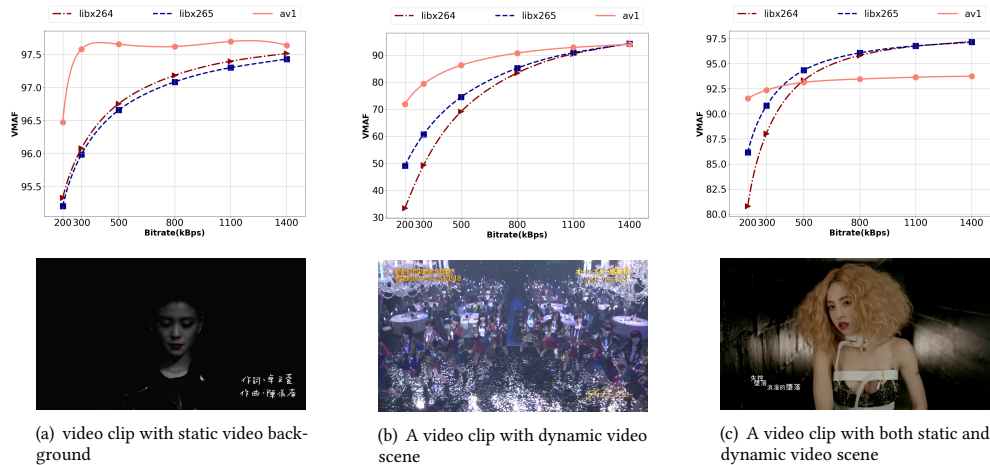


**Figure 1: This group of figures shows our motivation: In the real-time live streaming scenario, high video bitrate is equaled to high video quality, however, in some circumstance, high video quality only requires a low bitrate.**

neural network. The inputs of the VQRL are past time network status observed and future video quality predicted by VQPN, and the output is the bitrate for the next video with high video quality and low latency.

We design the training methodologies for those two neural networks respectively. To train VQPN, in addition to some general test video clips, we build up a dataset consisting of various types videos including movie, live-cast show, and music video(MV). For training VQRL, we propose an offline acceleration network simulator to emulate real-world network environment with a trace-driven dataset. We then collect a corpus of network traces for the simulator with both packet-level traces and chunk-level public traces.

After deciding the architecture of two neural networks, we compare QARC with existing proposed approaches, results of trace-driven emulation show that QARC outperforms with existing proposed approaches, with improvements in average video quality of 18% - 25% and decreases in average queuing delay of 23% - 45%. Besides that, by comparing the performance of QARC with the baseline which represents the offline optimal based on high bitrate and low latency over different network conditions and videos, we find that in all considered scenarios, despite a decrease in average video quality of only 4% - 9%, QARC saves the sending rate with 46% to 60% and reduces the average queuing delay of 40% to 50%.

As a result, our contributions are shown as follows.

- Unlike the previous goal, we propose a novel sight to evaluate QoE: aiming to optimize video quality rather than video bitrate during the entire video session.
- To the best of our knowledge, we are the first to establish a deep reinforcement learning (DRL) model to select sending bitrate for future video frames based on jointly considered perceptual video quality and network status observed in the real-time video streaming scenario.
- Due to the complexity of input state, we derive the neural network into two parts: the first part is a neural network used to precisely predict future video quality based on the previous video frames; the second part is an RL model used

to determine the proper bitrate based on the output of the first model. By using the output video quality from the first part instead of the raw video frames, the state space of the RL model can be reduced efficiently.

## 2 MOTIVATION

In this section, we start by designing two experiments to answer the following question: With the enhancement of video encoding technology, what will the correlation change between video quality and video bitrate?

- With the enhancement of video encoding technology, what will the correlation change between video quality and video bitrate?
- Can we precisely predict the fluctuation of the network without knowing the saturated bandwidth of the session?

### 2.1 High Video Quality or High Video Bitrate

To solve this, we establish a testbed to assess the video quality score of selected videos with the given encoding bitrate. The selected videos consist of three video clips, and each of them represents a video with static video scene (live-cast), a video with dynamic video scene (live concert), and a video with hybrid static video scene and dynamic video scene (MV) respectively.

In our experiment, we use Video Multi-Method Assessment Fusion(VMAF), a smart perceptual video quality assessment algorithm based on support vector machine(SVM) [21]. We compare the video quality score of each video in different encoders. In detail, we use three video encoders in our experiments including x264 [13], x265 [14], and AV1 [6]. The first two encoders are popularly used nowadays, and the last one is the state-of-the-art video encoder proposed by Google.

As illustrated in Figure 1, comparing VMAF score of different encoders on different videos and encoded bitrates, the results show that as the encode bitrate increases, the rate of increase in video quality score decreases. In addition, the refinement of encoder

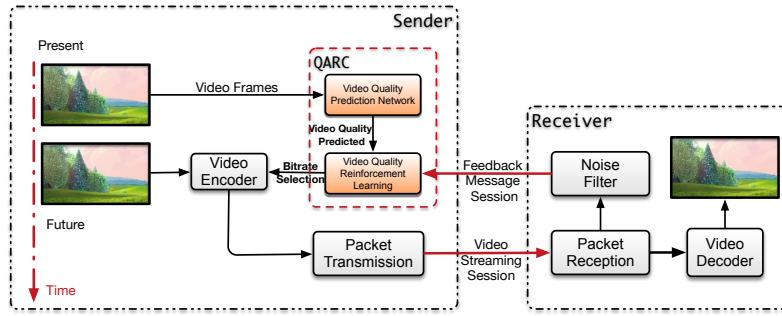


Figure 2: QARC's System Architecture

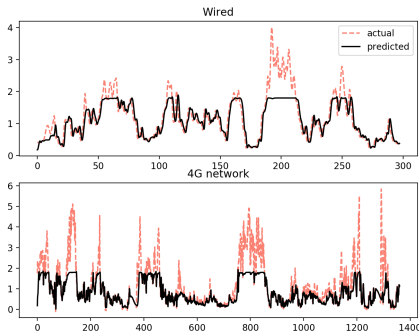


Figure 3: On-line Training

technology does not eliminate this phenomenon. As a result, in the real-time live streaming scenario, if we blindly select the high bitrate, it will make the burden of the network transmission highly increase with little enhancement of video quality.

Inspired by this, we propose a novel sight which aims to optimize perpetual video quality rather than video bitrate during the entire video session.

### 2.2 Estimate Future Network Status using Neural Network

The second issue is focused on conventional network congestion control. In the real-time network scenario, by using a neural network, how to accurately estimate the future saturated bandwidth based on past network status observed is still a challenge. In this paper, we use machine learning approach to solve the problem, and in details, we use online learning to train a neural network model to predict the future network status.

Considering past  $k$  time-slots, we define  $I_t = \{s, r, d\}$  as the input of neural network, where  $s$  is the sending rate of past  $k$  time-slots measured by the sender;  $r$  represents the receiving throughput collected by the receiver of past  $k$  time-slots, and  $d$  is the delay gradient computed by the receiver at that time-slot. In our experiment, we set  $k = 5$ . The output is a linear value described as the throughput of next time-slot  $t + 1$ , and in our problem, this value is equal to the available bandwidth. The model is mainly constructed as a 1D-convolutional network (1D-CNN). To train this model, We propose a network simulator which can use saturated traces to

generate network status data, and more details can be seen in Section 3.2. In particular, sending rate is constrained in the range of  $[0.01, 1.8]$  Mbps, which cannot reach the maximum size of available bandwidth.

Figure 3 illustrates our results on real-world network datasets (Section. 4.1). As shown, the model that is trained on the synthetic dataset is able to generalize across network conditions, and achieving SMAPE (Eq. 10) score within 11.1% of the model trained directly on the real-world networks including wired network and 4G network. These results suggest that, in practice, the neural network using 1d-CNN will have an ability to estimate future network status without measuring available bandwidth.

### 3 QARC'S MECHANISM

We start with introduce the conventional end-to-end transmission process for real-time video streaming. The system contains a sender and a receiver, and its transport protocol mainly consists of two channels: the streaming channel and the feedback message channel. At the beginning, the sender deploys a UDP socket channel to send the instant real-time video streaming packets  $P = \{p_0, p_1, \dots, p_k\}$ , denoted as a packet train [26], to the receiver through the streaming channel. The receiver then feeds network status observed back to the sender through the feedback channel. Based on this information, the sender will select bitrate for next time period.

As shown in Figure 2, on the basis of conventional real-time video streaming system architecture, we propose QARC, which is placed on the sender side. Motivated by the unbalanced growth of video quality and video bitrate as described in Section 2.1, we design a RL model to “learn” the correlation among the previous video frame, network status, and the best future bitrate. However, if we use raw pictures directly as its inputs, the state will cause “state explosion” [5]. Moreover, it will hard to train and validate in an allowable time. To overcome this, we meticulously divide the complexed RL model into two feasible and useful models, which involves:

**Video Quality Prediction Network(VQPN)**, proposed by end-to-end deep learning method, which predicts the future video quality metrics based on historical video frames;

**Video Quality Reinforcement Learning(VQRL)**, which uses A3C, an effective actor-critic method which trains two neural networks to select bitrates for future video frames based on network status observations and the future video quality metrics predicted by VQPN.

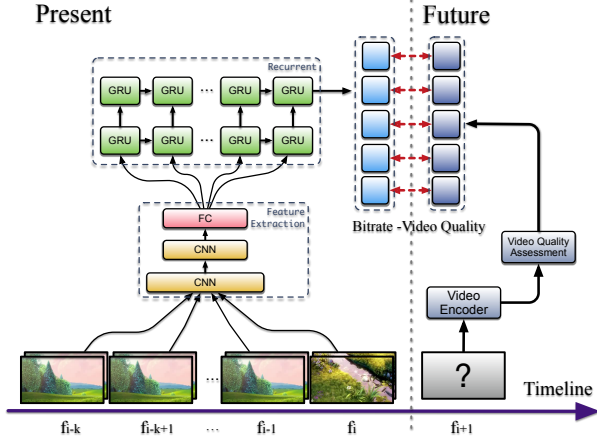


Figure 4: VQPN Architecture Overview

### 3.1 Video Quality Prediction Network(VQPN)

To help the RL model select a proper encoding bitrate for the next frame, we need to let the model “know” the relationship between the bitrate and corresponding video quality first. However, this form of prediction is quite challenging, because the perceptual video quality is closely related to the video itself. As shown in Figure 1, the video type, brightness, and objects number all have a great impact on the correlation between bitrate and VMAF. Motivated by the effectiveness of the neural network in a prediction of time sequence data, we design video quality prediction network(VQPN) helps the RL model to predict the perceptual video quality of the future frame. Figure 4 describes the VQPN’s neural network architecture, which is mainly made up with a layer that extracts image features through Convolutional Neural Network (CNN), and another layer which capture temporarily features via Recurrent Neural Network (RNN). Details are shown as follows.

**Video Quality Metric:** We use mean video quality metric to describe the quality of the video over a period. For each raw video frame  $f_i$  in time-slot  $t$ , the video quality score  $V_{f_i, bitrate}$  is computed by the raw video frames  $f$  and the bitrate at which the raw video frames  $f$  will be encoded, then the mean score  $V_{t, bitrate}$  is defined as the average value of  $V_{f, bitrate}$ . In our study, we use mean VMAF score, which is a score that is specifically formulated by Netflix to correlate strongly with subjective MOS scores to describe the video quality of video frames. In particular, we normalize the score into the distribution of the range from [0,1].

**Input:** VQPN takes state inputs  $F_i = [f_{i-k}, f_{i-k+1}, \dots, f_i]$  to its neural networks, where  $f_i$  represents the sampled video frame for the past  $i$  time period.

**Extract image features:** VQPN uses CNN layers to extract frame features, which can obtain the spatial information for each video frame in inputs  $F_i$ .

**Capture temporal features:** Upon extracting frame features, VQPN uses a double-layered recurrent layer [4] to further extract temporal characteristics of the video frames  $F_i$  in past  $k$  sequences.

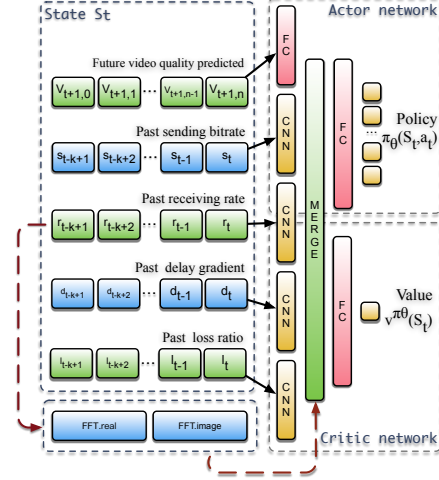


Figure 5: The Actor-Critic algorithm that VQRL uses to generate sending bitrate selection policies

**Output:** The outputs of VQPN are the prediction of the video quality assessment in the next time slot  $t + 1$  of candidate bitrates, denoted as  $V_{t+1}$ .

**Loss function:** We use mean square error(MSE) to describe the loss function, besides that, we also consider to add regulation to the loss function to decrease the probability of over fitting that on training set. Let  $\hat{V}_t$  denote the real vector of video quality score of the video in time  $t$ . Therefore, the loss function can be written as (Eq. 1):

$$L_t(V; \theta) = \frac{1}{N} \sum |V_t - \hat{V}_t|^2 + \lambda ||\theta||^2 \quad (1)$$

### 3.2 Video Quality Reinforcement Learning(VQRL)

In our study, we aim to let the neural network “learn” a video bitrate selection policy from observations instead of using preset rules in the form of fine-tuned heuristics. Specifically, our approach is based on RL. The sender, serving as an agent in RL problem, observes a set of metrics including future video quality and previous network status as the state. The neural network then selects the action as the output which denotes the video bitrate of next time-slot. Then the goal is to find the policy that maximizes the quality of experience (QoE) perceived by the user. In our scheme, QoE is influenced by video quality, latency, and smoothness.

As shown in Figure 5, We formulate “video quality first” real-time video streaming problem within A3C framework, named as video quality reinforcement learning (VQRL). Detailing our system components, which include:

**Input:** We consider the metrics which can be obtained by both sender and receiver from feedback message session. VQRL’s learning agent pushes the input state of time-slot  $t$   $s_t = \{s, r, d, l\}$  into neural network, where  $s$  is the video sending rate of the past  $k$  sequences which is equal to the throughput measurement from the uplink of the sender;  $r$  represents the receiving bitrate of past  $k$  sequences measured by the receiver;  $d$  is the delay gradient which is

measured between a sender and receiver of the recent  $k$  sequences;  $l$  is the packet loss ratio of the previous  $k$  sequences.

To better estimate the network condition in our scenario, we need precisely measure queuing delay of each packet. However, due to the clocks on both sides are unsynchronized, the measurements are unreliable. Motivated by [3], we also use delay gradient to solve the problem. More details can be seen in [3].

Besides that, we assume receiving bitrate as a form of signal. Then, the Fast Fourier Transform (FFT) can be used to decompose signals into a complex-valued function of frequency, whose absolute value represents the amount of that frequency present in the original function, whose complex argument is the phase offset of the basic sinusoid in that frequency. [7] As a result, we add the additional features into input which decomposed the receive rate sequence through FFT. The results that validate its improvement will be discussed in Section 4.2;

**Policy:** The agent needs to take action when receiving the state, and the policy is the guide telling the agent which action will be selected in the RL problem. In general, the action space is discrete, and the output of the policy network is defined as a probability distribution:  $f(s_t, a_t)$ , meaning the probability of selection action  $a_t$  being in state  $s_t$ . In this paper, the action space contains the candidate of sending bitrate in the next time-slot.

In traditional RL problem, the state space is small and can be represented in a tabular form, and there have been a lot of effective algorithms to solve this kind of problems, such as Q-learning and SARSA [28]. However, in our problem, the state space is fairly large, e.g., loss rate and received bit rate are continuous numbers, so it is impossible to store the state in a tabular form. To tackle this barrier, we use a neural network [10] to represent the policy, and the weights of the neural network, we use  $\theta$  in this paper, are called the policy parameters. In recent researches, the technique of combining neural network and RL is widely used to solve large-state-space RL problems [17, 27] and shows its exceptional power;

**Training:** In the RL problem, after taking a specific action in state  $s_t$ , the agent will get a corresponding reward, and the goal for the RL agent is to find the best action in each state which can maximize the accumulated reward  $r_t$  and as a result, the policy should be changed in the direction of achieving this goal. In this paper, we use A3C [18], a state of the art actor-critic RL algorithm, as the fundamental algorithm of our system, and in this algorithm, policy training is done by performing policy gradient algorithm.

The key thought of the policy gradient algorithm is to change the parameter in the direction of increasing the accumulated reward. The gradient direction is the direction in which a function increases. The gradient of the accumulated reward with respect to policy parameter  $\theta$  can be written as:

$$\nabla E_{\pi_{\theta}} \left[ \sum_{t=0}^{\infty} \gamma^t r_t \right] = E_{\pi_{\theta}} [\nabla_{\theta} \log \pi_{\theta}(s, a) A^{\pi_{\theta}}(s, a)] \quad (2)$$

and we can use:  $E_{\theta}[\nabla_{\theta} \log \pi_{\theta}(s, a) A^{\pi_{\theta}}(s, a)]$  as its unbiased form, where  $A(s_t, a_t)$  is called the advantage of action  $a_t$  in state  $s_t$  which satisfies the following equality:

$$A(a_t, s_t) = Q(a_t, s_t) - V(s_t) \quad (3)$$

where  $V(s_t)$  is the estimate of the value function of state  $s_t$  and  $Q(a_t, s_t)$  is the value of taking certain action at in state  $s_t$ , and it can also be written as:

$$Q(a_t, s_t) = r_t + \gamma V(s_{t+1} | \theta_{t+1}) \quad (4)$$

Thus, policy parameter will be updated as:

$$\theta \leftarrow \theta + \alpha \sum_t \nabla_{\theta} \log \pi_{\theta}(s_t, a_t) A(s_t, a_t) \quad (5)$$

in which the parameter  $\alpha$  represents the learning rate. To calculate  $A(s_t, a_t)$ , we need to have the  $V(s_t)$  first, and we can estimate it in the value network. The value network aims to give a reasonable estimate of the actual value of the expected accumulated reward of state  $s_t$ , written as  $V(s_t | \theta_v)$

Continuing the same line of thought, value network also uses neural network to represent the large state space. In this paper, we use n-step Q-learning to update the network parameter [18], and for each time, the error between estimation and true value can be represented as Eq.6:

$$Err_t = (r_t + \gamma V(s_{t+1} | \theta_v) - V(s_t | \theta_v))^2 \quad (6)$$

where  $V(s_t | \theta_v)$  is the estimate of  $V(s_t)$ , and to reduce the  $Err_t$ , the direction of changing parameter  $\theta_v$  is the negative gradient of it, and in A3C, the gradient will be added up with respect to  $t$ , so the value network will be updated as:

$$\theta_v \leftarrow \theta_v - \sum_t \nabla_{\theta_v} Err_t \quad (7)$$

where  $\alpha$  is the learning rate. Inspired by [17, 18], we also add the entropy of policy in the object of policy network, which can effectively discourage converging to suboptimal policies. See more details in [18]. So the update of the theta will be rewritten as:

$$\theta \leftarrow \theta + \alpha \sum_t \nabla_{\theta} \log \pi_{\theta}(s_t, a_t) A(s_t, a_t) + \beta \nabla_{\theta} H(\pi_{\theta}(\cdot | s_t)) \quad (8)$$

where  $\beta$  is also a hyper-parameter. After convergence, the value network will be abandoned, and we only use policy network to make decisions;

**Multiple training:** To accelerate the training process, as suggested by [18], we modify VQRL's training in the single agent as training in multi-agents. Multi-agents training consists of two parts, a central agent and a group of forwarding propagation agents. The forward propagation agents only decide with both policy and critic via state inputs and neural network model received by the central agent for each step, then it sends the  $n$ -dim vector containing  $\{state, action, reward\}$  to the central agent. The central agent uses the actor-critic algorithm to compute gradient and then updates its neural network model. Finally, the central agent pushes the newest model to each forward propagation agent. Note that this can happen asynchronously among all agents, for instance, there is no locking between agents. By default, VQRL with multiple training

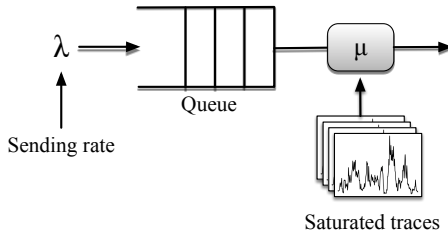


Figure 6: The working principle of the network simulator.

uses 8 forward propagation agents and 1 central agent;

**Train with network simulator:** To train VQRL, we first consider to train our neural network model in real-world network conditions, e.g., deploying the model on the edge server. With the increasing number of session, the model will finally converge. However, training the model online is hard to converge because RL training should meet almost all network status as the state. We then decide to train the model in simulated offline networks. Hence, we are facing new challenges: How to design a fast-forward network simulator which can precisely compute the latency with given saturated trace and sending rate?

To train our model, our training data should consist of queuing delay rather than one-way delay. So, our simulator should simulate the process of the packets coming and leaving in different network conditions, and keep track of the timestamps, by which we can get the corresponding queuing delay.

Inspired by [31] and [19], we use saturated network trace to generate queuing delay data. Seen in Figure 6, assuming the distribution of packets arrival and leave fits closely to the Poisson process [31], we use sending bitrate and bandwidth in saturated network traces as the arriving rate  $\lambda$  and leaving rate  $\mu$ , respectively.

In detail, we regard the channel link between the sender and the receiver as a single device, and queuing delay the device generates is called 'self-inflicted delay' [31]. The device consists of three queues, named as 'input' 'output' and 'limbo'. An algorithm is designed to release packets from each queue based on the corresponding packet-level delivery trace. Each element in the queue is the opportunity of packet-delivery, which means, the time(in milliseconds) at which an MTU-sized packet will be delivered. For each period  $(t1, t2]$ , the offline-network simulator compare the timestamp of the front packet in 'input' with that in 'limbo'. If timestamp in 'input' queue is bigger than or equal to the one in 'limbo', the simulator will push the front packet into the bottom of the 'output' queue, and then computes the delay gradient between the two packets. On the contrast, the delivery opportunities will be wasted if the timestamp in 'input' queue is smaller than that one in 'limbo' queue. The simulator only pops the front packet in 'limbo' queue. By this process, the simulator returns mean self-inflicted delay and total bytes that the sum of 'output' queue every interval  $T$ .

## 4 EVALUATION

### 4.1 Datasets and Metrics

**Video dataset:** We train and test VQPN on two video datasets, that is, VideoSet: a large-scale compressed video quality dataset based

on JND measurement and self-collected video datasets: a video quality dataset involves live-casts, music-videos, and some short movies. For each video in datasets, we measure its VMAF with the bitrate of 300kbps to 1400kbps, and the reference resolution is configured as  $800 \times 480$ , which is the same size as default resolution that observed by the receiver during the real-time live streaming. We generate the VMAF video datasets using both x264 and x265 encoder.

**Network traces:** To train and evaluate VQRL, the first thing we must do is to generate saturated network trace datasets. However, these types of network traces are hard to be recorded, even public datasets are extremely limited. For example, Cellsim [31] only provides a small number of saturated network traces which describe the cellular network conditions instead of all network environments, which hardly afford us to make our neural network converge. Thus, we consider to collect datasets in two ways:

- **Packet-level network traces:** We use a proprietary dataset of packet-level live-cast session status from all platforms APPs of Kwai collected in January 2018. <sup>1</sup> Motivated by the one-way-delay estimation method in Ledbat [25], We generate 2,300 real network traces from packet train datasets.
- **Chunk-level network traces:** We also collect hybrid network traces datasets which consists of different network datasets, such as FCC [23] and Norway [24]. The FCC dataset is a broadband dataset, and Norway dataset is mainly collected in 3G/HSDPA environment. In short, we generate 1,000 network traces from the datasets.
- **Synthetic network traces:** We generate a synthetic dataset using a Markovian model where each state represented an average throughput in the aforementioned range.[17] Thus, we create a dataset in over 500 traces which can cover a board set of network conditions.

**QoE metrics:** For a better result, we consider designing Quality of Experience (QoE) metric based on previous scheme. In the recent research[ref][ref][ref], QoE metrics are evaluated as a method with 4 essential factors: bitrate received, loss ratio, latency, and delay gradient, with no considering video quality metric. Still, in this paper, after rethinking the correspondence between video quality and video bitrate, we redefine the QoE metric as (Eq. 9)

$$QoE = \sum_{n=1}^N (V_n - \alpha B_n - \beta D_n) - \gamma \sum_{n=1}^{N-1} |V_n - V_{n-1}| \quad (9)$$

for a live video with  $N$  time-slots. Where  $V_n$  denotes the video quality of time  $n$ ,  $B_n$  is the video bitrate that the sender selects, and  $D_n$  represents the delay gradient measured by the receiver. The final term comprises the smoothness of video quality. Coefficient  $\alpha$ ,  $\beta$  and  $\gamma$  are the weight to describe their aggressiveness.

### 4.2 Implementation

We now describe the implementation of QARC<sup>2</sup>. In this section, we decide the best hyper-parameters and explain the implementation of VQPN and VQRL respectively.

<sup>1</sup>Kwai is a leading platform in China which has over 700 million users worldwide, and millions of original videos are published on it every day.

<sup>2</sup>The neural network construction details can be found at GitHub.

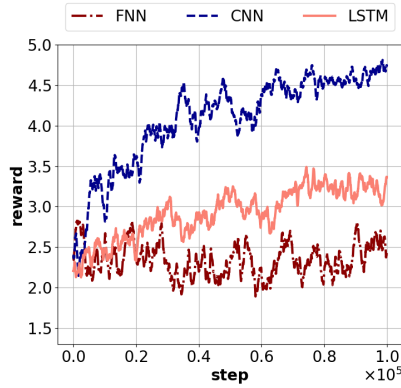


Figure 7: Comparing the performance as different neural network model including CNN, FNN, and GRU.

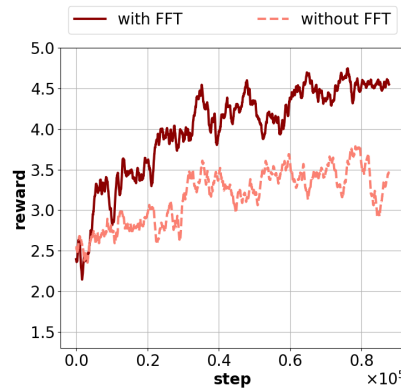


Figure 8: Comparing VQRL which uses FFT with the one without using it.

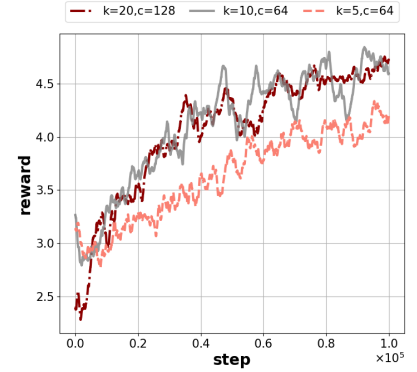


Figure 9: Sweeping sequence length and number of filters in VQRL's neural network architecture.

filter number	hidden units	Learning Rate			
		1e-3	1e-4	1e-5	6e-6
32	32	4.88	5.20	4.42	4.24
32	128	4.40	4.28	4.24	4.13
64	64	3.94	3.73	4.22	4.31
64	128	4.92	4.17	4.16	4.17
<b>128</b>	<b>64</b>	4.20	<b>3.41</b>	4.17	4.23
128	128	4.52	3.86	4.15	3.99

Table 1: Comparing performance (SMAPE%) of VQPN with different filter number and hidden units. Results are collected under learning rate=1e-3,1e-4,1e-5, and 6e-6 respectively.

**Time-slot t:** In this paper, we set time-slot  $t$  to 1s.

**VQPN:** The introduced VQPN help VQRL predict future video quality, but we have yet studied how to set the hyper-parameters. Table 1 shows our results with different settings of filter number, hidden units, and learning rate. Results are summarized as symmetric mean absolute percentage error (SMAPE) metric, which is computed as Eq. 10:

$$\text{SMAPE} = \frac{100\%}{n} \sum_{t=1}^n \frac{|F_t - A_t|}{(|A_t| + |F_t|)/2} \quad (10)$$

where  $A_t$  is the actual value and  $F_t$  is the forecast value. Empirically, filter number = 128, hidden units = 64, and learning rate = 1e-4 yields the best performance.

To sum up, VQPN passes  $t = 5$  past time video, and it samples 5 frames for each time, totally  $k = 25$  previous frames as input to the neural network architecture, and each size of the frame is defined as [64,36] with 3 channels. The input frames then extract features in 128-dimension vector via a feature extraction layer respectively. The feature extraction layer is constructed with 5 layers, a convolution layer with 64 filters, each of size 5 with stride 1, an average pooling layer with filter number  $3 \times 3$ , another convolution layer with 64 filters, each of size 3 with stride 1, also, an max pooling layer with filter number  $2 \times 2$ . Finally, the feature extraction layer passes the features into a hidden layer with 64 neurons.

Considering the frame sequence as a time series data, a recurrent network is designed to estimate future video quality. VQN passes  $k = 25$  feature maps to a gated recurrent unit (GRU) layer with 64 hidden units, then the states of that layer are passed to another GRU layer with the same hidden units. A hidden layer is then connected to the hidden output of the last GRU layer. Finally, VQPN uses the final output as a 5-dimension vector, and for each value in the vector represents the video quality score of video bitrate {300, 500, 800, 1100, 1400} kbps.

During the training process, we use Adam gradient optimizer to optimize VQPN with learning rate  $\alpha = 10^{-4}$ . In this work, we use TensorFlow [1] to implement this architecture, in particular, we leveraged the TFLearn deep learning library's TensorFlow API to declare VQPN.

**VQRL:** In this section, we describe how to choose the best neural network model of VQRL. Firstly, we design three different models which are based on FNN (Feedback Neural Network), CNN (Convulsion Neural Network), and LSTM (Long-Short Term Memory) respectively. We set sequence length  $k = 5$ . We use the QoE metric with  $\alpha = 0.2$ ,  $\beta = 1.0$  and  $\gamma = 1.0$  as the baseline reward. As illustrated in Figure 7(a), the CNN model increase the average QoE by about 39% compared with the LSTM model and about 83% compared with the FNN model.

Then, we consider validating the importance of adding FFT feature into inputs. We set up two CNN models, one of them is established with FFT feature. We set sequence length  $k = 20$  with the same environment as the first experiment. Results are shown in Figure 8(b), which implies that the CNN model with using FFT feature can provide a high reward with the improvement of about 29% compared with the CNN model without using FFT feature.

Finally, we investigate how CNN parameters inflect output results. In our experiment, the different parameters are set as  $\{k = 5, c = 64\}$ ,  $\{k = 10, c = 64\}$  and  $\{k = 20, c = 128\}$ , in which  $k$  is the input sequence length and  $c$  is the CNN channel size. As shown in Figure 9(c), with the increase of  $k$  and  $c$ , the performance increases. However, when we choose parameter  $\{k = 20, c = 128\}$ , the average QoE only increases 1% compared with parameter  $\{k = 10, c = 128\}$ ,

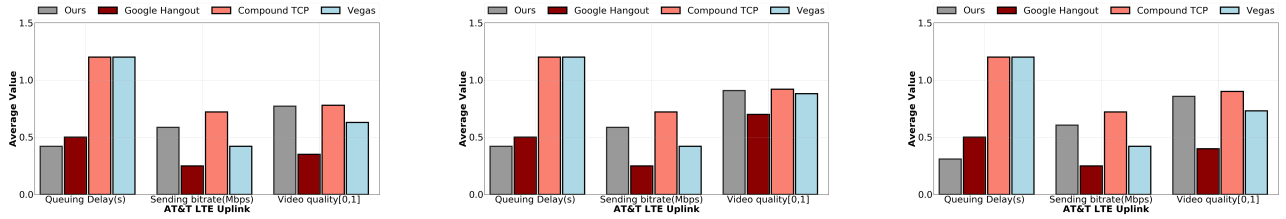


Figure 10: Comparing QoE with previous proposed approaches on the 4G network environments: The QoE of QARC is considered as  $\alpha = 0.2, \beta = 10.0,$  and  $\gamma = 1.0$ . After testing three video clips, results are shown as average queuing delay, average sending rates, and average video quality.

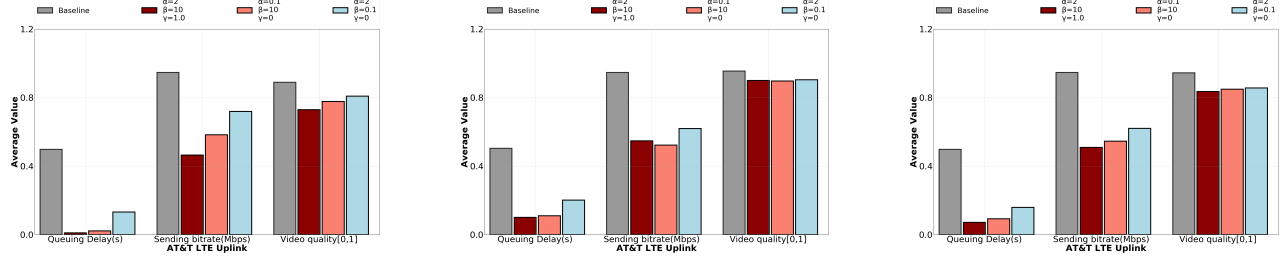


Figure 11: Comparing QoE with different QoE and the baseline which is computed as an offline optimal value based on high video bitrate. We evaluate several QARC methods and a baseline on the boardband network environments. Like the process of Figure 10, after testing three video clips, results are shown as average queuing delay, average sending rates, and average video quality which are against the performance of the baseline value.

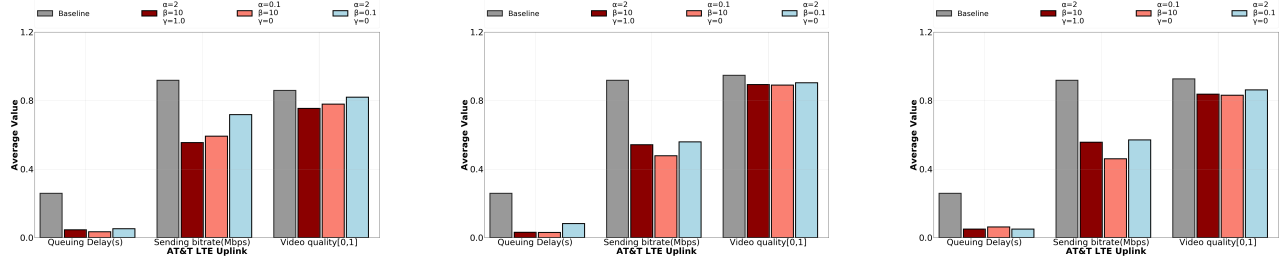


Figure 12: Like the process of Figure 11, comparing QoE with different QoE and the baseline which is computed as an offline optimal value based on high video bitrate. We evaluate several QARC methods and a baseline on the 4G network environments.

so in consideration of calculation complexity, we finally choose  $\{k = 10, c = 64\}$ . Additionally, the action space is configured as 5, which is same as the output of VQPN. During the training process, we use Adam gradient optimizer to optimize it, and the learning rate for the actor and critic is set as  $6.75 \times 10^{-4}$  and  $10^{-3}$ , respectively.

**Training time:** To measure the performance limitation of predicting future video quality, we profile VQPN’s training process. To know when the network converges, we use early stopping method to train the neural network. Totally, training VQPN requires approximately an hour on a single GPU GTX-1080Ti.

For measuring the overhead of the neural network of VQRL, we also introduce the training process for it. To train this, we use 8 agents to update the parameters of the central agent in parallel. The neural network will converge in 22 hours, or less than 5 hours using 20 agents<sup>3</sup>.

<sup>3</sup>This experiment is worked on Azure with an instance in 25 CPUs and 140G RAM size.

### 4.3 Experiments and Results

In this section, we establish a real-time video streaming system to experimentally evaluate QARC. Our results answer the following questions:

- (1) Comparing QARC with previously proposed approaches in different video clips, is QARC the best?
- (2) Compared with the baseline algorithm based on high video bitrate and low latency, how much improvement does QARC gain on the results?
- (3) How does the coefficient  $\alpha, \beta,$  and  $\gamma$  affect the outcome of QARC?
- (4) How does QARC perform in the real-world network conditions?

**QARC vs. Existing approaches** In this experiment, we evaluate QARC with existing proposed methods on several network traces which represents various network conditions. After running the trace for each approach, we collect the average queuing delay, average from the receiver. We compare their performance to different video clips. In this experiment, QARC is compared with Google



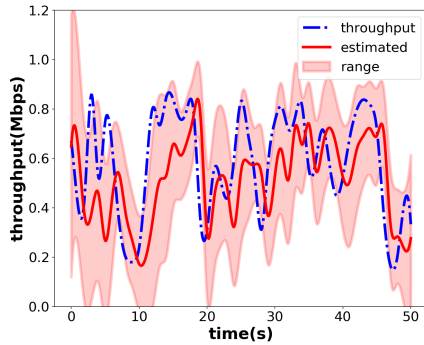


**Figure 13: Comparing the accuracy with neural network using range and without using it. The result shows that estimating throughput in range can be more conducive to describe the future observations.**

Hangout, a famous video conference app, Compound TCP[9], and Vegas [2]. As illustrated in Figure 10, one of the results show that QARC outperforms with existing proposed approaches, with improvements in average video quality of 18% - 25% and decreases in average queuing delay of 23% - 45%. Especially, we obtain that QARC also saves the sending rate, which also performs well.

**Video quality first vs. Bitrate first** We aim to evaluate QARC with different QoE parameters and the baseline algorithm which uses the policy based on high video bitrate. Specifically, we compare QARC to the baseline algorithm in terms of queuing delay, the sending rate, and the video quality of the entire video session.

As shown in Figure 11 and Figure 12, compared with the baseline algorithm on broadband and 4G network environments, the performance of QARC outperforms the baseline based on greedy algorithm. In the broadband network environment, despite a shrinkage in average video quality of 4% - 9%, QARC decreases the sending rate of 46% to 60% and reduces the average queuing delay<sup>4</sup> from 0.5s to 0.04s. It is noteworthy that if the footage of the video does not switch violently (Figure 11(b)), for instance, in video conference scenario, sending bitrate decreases from 51% to 62% while video quality reduces less than 5%. We can also find similar results in 4G network environments, and details can be seen in Figure 11.

**Influence of  $\alpha, \beta$  and  $\gamma$ :** Figure 11 and Figure 12 show the results of QARC with different initial QoE reward parameters. Unsurprisingly, initialize QoE reward with small latency coefficient  $\alpha$  yield high-performance improvement over the one with a bigger  $\alpha$  in wired network conditions, however, in 4G network environments, it performs a very different performance. In conclusion, there is no optimal pair can fit any network conditions.

**QARC in the real-world network:** We evaluated QARC and several state-of-the-art ABR algorithms in the wild using three different networks: the Verizon LTE cellular network, a public WiFi

<sup>4</sup>In this paper, queuing delay is regarded as self-inflicted delay, which is a lower bound on the 95% end-to-end delay that must be experienced between a sender and receiver, given observed network behavior. [31]

network at a local coffee shop, and the wide area network between Shanghai and Boston. In these experiments, a client, running on a Macbook Pro laptop, contacted a video server running on a desktop machine located in Boston. We considered a subset of the ABR algorithms listed in Section 5.1: WebRTC, Skype and QARC. On each network, we loaded our test video ten times with each scheme, randomly selecting the order among them. The QARC ABR algorithm evaluated here was solely trained using the broadband and HSDPA traces in our corpus. However, even on these new networks, QARC was able to outperform the other schemes on the QoE metric (Figure 11). Experiments with the other QoE metrics show similar results.

## 5 RELATED WORK

### 5.1 Real-time rate control methods

**loss-based:** Loss-based approaches such as TFRC [11] and rate adaptation protocol (RAP) [22], have been widely used in TCP congestion control, and these methods increase bitrate till packet loss occurs, which means that the actions are always late, because when packet loss occurs, latency also increases. Furthermore, using packet loss event as the control signal may cause its throughput to be unstable, especially in error-prone environments [8].

**delay-based:** Delay-based approaches, try to adjust sending rate to control the transmission delay, can be divided into the end-to-end delay (RTT) approaches, such as TCP Vegas [2]; one-way delay approaches, such as LEDBAT (Over UDP) and TCP-LP [16, 25], and delay gradient approaches [3]. However, it is hard for the delay metrics to converge to the target value in some network conditions in which its upper limit has always suffered a wide range of changes, such as WiFi [8, 20].

**rate-based:** This approach controls the bitrate using the bandwidth estimation method which motivated by the adaptive filter algorithm. A large scale of adaptive filter algorithm has been used in bandwidth estimation, such as ARIMA(), RLS(), Kalman Filter, and so forth. The key limitation of this approach is shown as follows: 1. the result of bandwidth-based approach largely depends on the accuracy of bandwidth estimation method 2. the adaptive filter algorithm estimates the bandwidth by using fixed initial parameters which fits the specific network conditions, thus, it doesn't have an ability to adapt to all network status.

**QoS-based:** QoS-based bitrate control method, such as Rebera [15] and GCC [3], they control sending bitrate based on previous network status observed including end-to-end latency, receiving rate which is measured by the receiver, and past sending bitrate, loss ratio which is measured by the sender.

### 5.2 Video Quality Metrics

Video quality is a characteristic to measure the perceived video degradation while passing through a video transmission system. Up to now, the video quality metrics which are commonly used are shown as follows.

**PSNR:** A traditional signal quality metric [12], which is directly derived from mean square error (MSE) or its square root (RMSE). Due to the simplicity and low complexity of its calculation, PSNR continues to be the most popular evaluation of the video quality.

However, the result cannot precisely reflect the visual quality seen by human eyes.

**SSIM:** An image quality metric, submitted in 2004 by Wang et al. [29]. Unlike previously proposed video quality evaluation criteria, SSIM uses the structural distortion measurement instead of mean square error. Due to the consideration of the whole picture, SSIM can give a proper evaluation of the video quality experienced by users. However, SSIM is not a professional tool for video quality assessment.

**VMAF:** Video Multi-method Assessment Fusion (VMAF) [21] is an objective full-reference video quality metric which is formulated explicitly by Netflix to estimate subjective video quality based on a reference and distorted video sequence. Using machine learning techniques, VMAF provides a single output score in the range of [0, 100] per video frame. In general, this metric is focused on describing the quality degradation due to compression and rescaling and it is closer to people's real experience of video quality than previous schemes.

### 5.3 Deep Reinforcement Learning in the network approach:

**Remy:** Remy [30] decides with "a tabular method", and it collects experience from the network simulator with network assumptions, however, like all TCP variants, when the real network deviates from Remy's input assumption, performance degrades.

**Pensieve:** Mao et al. [17] develop a system that uses deep reinforcement learning to select bitrate for future video chunks. Unlike most of the adaptive bit rate (ABR) algorithms, Pensieve does not need any predefined rules and assumptions to make decisions, and it can automatically adjust itself to the change of network conditions. By comparing with the existing ABR algorithms, Pensieve performs very well.

## 6 CONCLUSION

In this paper, we propose QARC, a deep-learning based rate control algorithm in the real-time live streaming scenario. Unlike previously proposed approaches, we try to get a higher video quality with possibly lower sending rate. Due to that fixed rules cannot effectively handle the complicated scenarios caused by perplexing network conditions and various video content, we use deep reinforcement learning to select the future video bitrate, which can adjust itself automatically to the change of its inputs. To reduce the state space of the reinforcement learning model, we derive the neural network into two parts and train them respectively. After training on a board set of network data, we explore the performance of QARC over several network conditions and QoE metrics. We find that QARC outperform existing rate control algorithms by 18% - 25% in average video quality.

Additional research may focus not only on the real-time live streaming scenario but also in 360° video streaming.

## REFERENCES

- [1] Martín Abadi, Paul Barham, Jianmin Chen, Zhifeng Chen, Andy Davis, Jeffrey Dean, Matthieu Devin, Sanjay Ghemawat, Geoffrey Irving, Michael Isard, et al. 2016. TensorFlow: A System for Large-Scale Machine Learning. In *OSDI*, Vol. 16. 265–283.
- [2] Lawrence S. Brakmo and Larry L. Peterson. 1995. TCP Vegas: End to end congestion avoidance on a global Internet. *IEEE Journal on selected Areas in communications* 13, 8 (1995), 1465–1480.
- [3] Gaetano Carlucci, Luca De Cicco, Stefan Holmer, and Saverio Mascolo. 2016. Analysis and design of the google congestion control for web real-time communication (WebRTC). In *Proceedings of the 7th International Conference on Multimedia Systems*. ACM, 13.
- [4] Junyoung Chung, Caglar Gulcehre, Kyunghyun Cho, and Yoshua Bengio. 2014. Empirical Evaluation of Gated Recurrent Neural Networks on Sequence Modeling. *arXiv: Neural and Evolutionary Computing* (2014).
- [5] Edmund M. Clarke, William Klieber, Miloš Nováček, and Paolo Zuliani. 2012. *Model Checking and the State Explosion Problem*. Springer Berlin Heidelberg, Berlin, Heidelberg, 1–30. [https://doi.org/10.1007/978-3-642-35746-6\\_1](https://doi.org/10.1007/978-3-642-35746-6_1)
- [6] Alliance for Open Media. 2018. AV one encoder. <https://aomedia.org/>. (2018).
- [7] Matteo Frigo. 1999. A fast Fourier transform compiler. *programming language design and implementation* 34, 5 (1999), 169–180.
- [8] Yufeng Geng, Xinggong Zhang, Tong Niu, Chao Zhou, and Zongming Guo. 2015. Delay-constrained rate control for real-time video streaming over wireless networks. In *Visual Communications and Image Processing (VCIP), 2015*. IEEE, 1–4.
- [9] Sangtae Ha, Injong Rhee, and Lisong Xu. 2008. CUBIC: a new TCP-friendly high-speed TCP variant. *ACM SIGOPS operating systems review* 42, 5 (2008), 64–74.
- [10] Martin T Hagan, Howard B Demuth, Mark H Beale, et al. 1996. *Neural network design*. Vol. 20. Pws Pub. Boston.
- [11] Mark Handley, Sally Floyd, Jitendra Padhye, and Jörg Widmer. 2002. *TCP friendly rate control (TFRC): Protocol specification*. Technical Report.
- [12] Alain Hore and Djemel Ziou. 2010. Image Quality Metrics: PSNR vs. SSIM. (2010), 2366–2369.
- [13] MulticoreWare Inc. 2006. x264 encoder. <https://x264.org/>. (2006).
- [14] MulticoreWare Inc. 2015. x265 encoder. <https://x265.org/>. (2015).
- [15] Eymen Kurdoglu, Yong Liu, Yao Wang, Yongfang Shi, ChenChen Gu, and Jing Lyu. 2016. Real-time bandwidth prediction and rate adaptation for video calls over cellular networks. In *Proceedings of the 7th International Conference on Multimedia Systems*. ACM, 12.
- [16] Aleksandar Kuzmanovic and Edward W Knightly. 2006. TCP-LP: low-priority service via end-point congestion control. *IEEE/ACM Transactions on Networking (TON)* 14, 4 (2006), 739–752.
- [17] Hongzi Mao, Ravi Netravali, and Mohammad Alizadeh. 2017. Neural adaptive video streaming with pensieve. In *Proceedings of the Conference of the ACM Special Interest Group on Data Communication*. ACM, 197–210.
- [18] Volodymyr Mnih, Adria Puigdomenech Badia, Mehdi Mirza, Alex Graves, Timothy Lillicrap, Tim Harley, David Silver, and Koray Kavukcuoglu. 2016. Asynchronous methods for deep reinforcement learning. In *International Conference on Machine Learning, 1928–1937*.
- [19] Ravi Netravali, Anirudh Sivaraman, Somak Das, Ameesh Goyal, Keith Winstein, James Mickens, and Hari Balakrishnan. 2015. Mahimahi: accurate record-and-replay for HTTP. (2015), 417–429.
- [20] K. Nihei, H. Yoshida, N. Kai, D. Kanetomo, and K. Satoda. 2017. QoE maximizing bitrate control for live video streaming on a mobile uplink. In *2017 14th International Conference on Telecommunications (ConTEL)*. 91–98. <https://doi.org/10.23919/ConTEL.2017.8000044>
- [21] Reza Rassool. 2017. VMAF reproducibility: Validating a perceptual practical video quality metric. In *Broadband Multimedia Systems and Broadcasting (BMSB), 2017 IEEE International Symposium on*. IEEE, 1–2.
- [22] R. Rejaie, M. Handley, and D. Estrin. 1999. RAP: An end-to-end rate-based congestion control mechanism for realtime streams in the Internet. In *INFOCOM '99. Eighteenth Annual Joint Conference of the IEEE Computer and Communications Societies. Proceedings. IEEE*, Vol. 3. 1337–1345 vol.3. <https://doi.org/10.1109/INFCOM.1999.752152>
- [23] Measuring Fixed Broadband Report. 2016. Raw Data Measuring Broadband America 2016. <https://www.fcc.gov/reports-research/reports/measuring-broadband-america/raw-data-measuring-broadband-america-2016/>. (2016). [Online; accessed 19-July-2016].
- [24] Haakon Riiser, Paul Vigmstad, Carsten Griwodz, and Pal Halvorsen. 2013. Commute path bandwidth traces from 3G networks: analysis and applications. (2013), 114–118.
- [25] Dario Rossi, Claudio Testa, Silvio Valenti, and Luca Muscariello. 2010. LEDBAT: The New BitTorrent Congestion Control Protocol. In *ICCCN*. 1–6.
- [26] Natsuhiko Sato, Takashi Oshiba, Kousuke Nogami, Anan Sawabe, and Koza Satoda. 2017. Experimental comparison of machine learning-based available bandwidth estimation methods over operational LTE networks. In *Computers and Communications (ISCC), 2017 IEEE Symposium on*. IEEE, 339–346.
- [27] David Silver, Aja Huang, Chris J Maddison, Arthur Guez, Laurent Sifre, George Van Den Driessche, Julian Schrittwieser, Ioannis Antonoglou, Veda Panneershelvam, Marc Lanctot, et al. 2016. Mastering the game of Go with deep neural networks and tree search. *nature* 529, 7587 (2016), 484–489.

- [28] Richard S Sutton and Andrew G Barto. 1998. *Reinforcement learning: An introduction*. Vol. 1. MIT press Cambridge.
- [29] Zhou Wang, A. C. Bovik, H. R. Sheikh, and E. P. Simoncelli. 2004. Image quality assessment: from error visibility to structural similarity. *IEEE Transactions on Image Processing* 13, 4 (April 2004), 600–612. <https://doi.org/10.1109/TIP.2003.819861>
- [30] Keith Winstein and Hari Balakrishnan. 2013. TCP ex machina: computer-generated congestion control. *acm special interest group on data communication* 43, 4 (2013), 123–134.
- [31] Keith Winstein, Anirudh Sivaraman, and Hari Balakrishnan. 2013. Stochastic forecasts achieve high throughput and low delay over cellular networks. (2013), 459–471.